# Hybrid Unified Kalman Tracking Algorithms for Heterogeneous Wireless Location Systems

Cheng-Tse Chiang, Po-Hsuan Tseng, *Student Member, IEEE*, and Kai-Ten Feng, *Member, IEEE*

***Abstract*—Location estimation and tracking for mobile stations have attracted a significant amount of attention in recent years. Different types of signal sources are considered available to provide measurement inputs for location estimation and tracking in heterogeneous wireless networks. Various techniques have been studied and combined for location tracking, e.g., the least square methods for location estimation associated with the Kalman filters for location tracking. In this paper, the hybrid unified Kalman tracking (HUKT) technique is proposed to provide an integrated algorithm for precise location tracking based on both time of arrival (TOA) and time difference of arrival (TDOA) measurements. A new variable is incorporated as an additional state within the Kalman filtering formulation to consider the nonlinear behavior in the measurement update process. The relationship between this new variable and the desired location estimate is applied in the state update process of the Kalman filter. Three different designs of hybrid factor are proposed to adaptively adjust the weighting value between the TOA and TDOA measurements. Moreover, similar concepts are also utilized in the design of unified Kalman tracking schemes for pure TOA and TDOA measurement inputs in this paper. Compared with existing schemes, numerical results illustrate that the proposed HUKT algorithm can achieve enhanced accuracy for mobile location tracking, particularly under environments with an insufficient number of measurements in one of the signal paths.**

***Index Terms*—Kalman filter, mobile location estimation and tracking, time difference of arrival (TDOA), time of arrival (TOA).**

## I. Introduction

WIRELESS location technologies, which are designed to estimate and track the position of a mobile station (MS), have drawn a lot of attention over the past few decades. Self-navigation and target tracking are the two main applications. With the acquisition of the MS's location information, different types of location-based services (LBSs) can be explored, including enhanced 911 (E-911) subscriber safety services [2], location-based billing, navigation systems, and applications for intelligent transportation systems [3]. Due to the emergent interests in LBSs, it is required to provide enhanced precision in location estimation and tracking of the MS under different types of environments.

A variety of localization techniques have been investigated and proposed in wireless standards [4]. Network-based location estimation schemes are widely employed in wireless communication systems. These schemes locate the position of an MS based on the measured radio signals from either its neighborhood base stations (BSs) in cellular networks or anchor nodes in wireless sensor networks (WSNs) [5], [6]. For convenience, these signal sources are represented as BSs in this paper. The location estimation algorithms can be categorized into range-free and range-based techniques. The range-free schemes [7]–[9] utilized the status of network connectivity between MS and BSs for localization, which possesses the benefits of simplicity and low cost. These schemes are primarily adopted in WSNs with the features of limited computation power and less requirement on positioning accuracy. On the other hand, to provide precise location estimation, range-based schemes are considered, which include received signal strength (RSS) [10], angle of arrival (AOA) [11], time of arrival (TOA) [12], and time difference of arrival (TDOA) [13]. The RSS schemes record the incoming signal strength from different wireless BSs for converting to distance measurement, and the AOA methods are in general implemented at the BSs to observe the signal bearing via the antenna array. The TOA schemes measure the arrival time of the radio signals coming from the BSs, whereas the TDOA algorithms measure the time difference between the radio signals.

One of the important issues for range-based positioning is its inherent nonlinear feature for location estimation, which results in complex computation and difficulties for analysis. Recursive Bayesian estimation [14]–[16] computes the posterior probability density function of the state variables based on both the incoming measurement inputs and the Markov state model recursively over time. With the estimated posterior probability density function, either the minimum mean square error (MMSE) or the maximum *a posteriori* estimation can be calculated. The Kalman filter is one of the simplest methods for Bayesian estimation and is proved to be an optimal realization of MMSE under the linear model perturbed by Gaussian noises [14]. Although the signal and noise are not jointly Gaussian, it is still considered an optimal linear MMSE (LMMSE) estimator. Moreover, the operation of the Kalman filter [16]–[18]

Manuscript received May 29, 2011; revised October 10, 2011; accepted November 18, 2011. Date of publication December 21, 2011; date of current version February 21, 2012. This work was supported in part by the Aiming for the Top University and Elite Research Center Development Plan under Grant NSC 99-2628-E-009-005, Grant NSC 98-2221-E-009-065, and Grant NSC 98-2917-I-009-110, by the MediaTek Research Center at National Chiao Tung University, and by the Telecommunication Laboratories at Chunghwa Telecom Co. Ltd., Taiwan. This paper was presented in part at the IEEE 21st International Symposium on Personal, Indoor, and Mobile Radio Communications, Istanbul, Turkey, September 2010. The review of this paper was coordinated by Prof. Dr. Y. Gao.

C.-T. Chiang and P.-H. Tseng were with the Department of Electrical Engineering and Control Engineering, National Chiao Tung University, Hsinchu 30010, Taiwan (e-mail: henrychiang.cm97g@nctu.edu.tw; walker.cm90@nctu.edu.tw).

K.-T. Feng is with the Department of Electrical Engineering and Control Engineering, National Chiao Tung University, Hsinchu 30010, Taiwan (e-mail: ktfeng@mail.nctu.edu.tw).

Color versions of one or more of the figures in this paper are available online at http://ieeexplore.ieee.org.

Digital Object Identifier 10.1109/TVT.2011.2180939

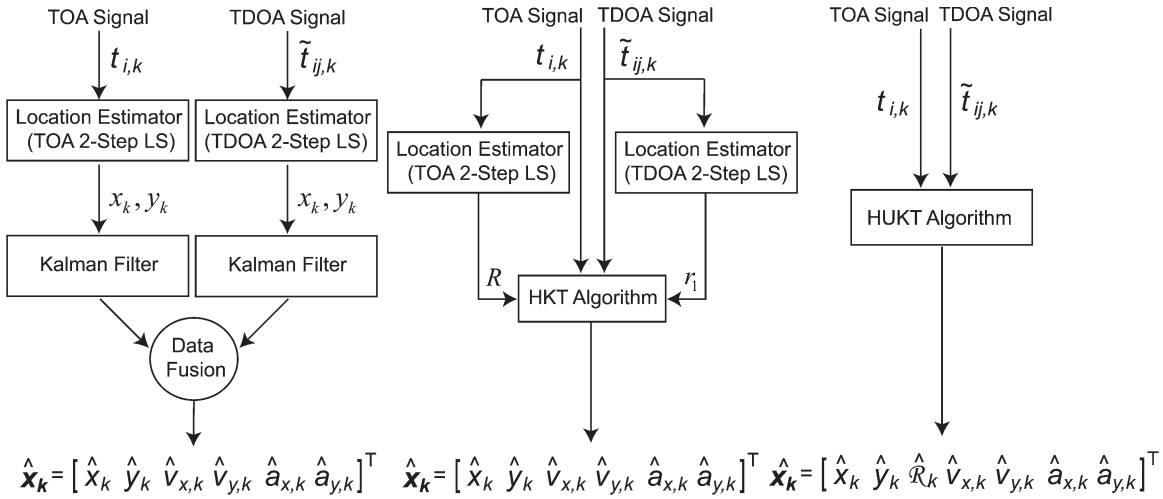


Fig. 1. (Left) HCLT scheme. (Middle) HKT scheme. (Right) Proposed HUKT scheme.

is linear, which offers efficient computation for real-time implementation. In [19] and [20], the Kalman filer has been extensively utilized to further enhance the precision for location estimation. It provides the estimation of internal states with dynamic weighting adjustment between the prediction and the observation input in recursion form. This feature alleviates the estimation outputs from severe signal variations and can finally converge to the true value. Several researches have adopted the Kalman filter to track the MS's position with considerations of the nonline-of-sight (NLOS) interferences [21] and the mobility information of moving MS [22], [23]. Compared with the methods for stationary location estimation, these tracking schemes take advantage of the previous location and movement of the MS, which can result in a smoothed MS trajectory with better estimation accuracy.

On the other hand, owing to the feasibility of providing synchronization between cellular BSs, the TDOA measurements have been extensively adopted for location estimation and tracking in existing telecommunication systems, e.g., the WiMax [24] standard. However, in urban canyons problem, it has been observed that the number of received Global Positioning System or cellular signals is insufficient for location estimation due to signal blockage in urban environment. Moreover, the study in [25] suggests the adoption of TOA-based signal sources for dedicated short-range communications (DSRC) to avoid the complex infrastructure required for TDOA measurements. To provide feasible precision for location estimation, it is sensible to combine these two types of signal sources under a variety of environments, e.g., to additionally include TOA-based sensor anchors or roadside DSRC devices with TDOA-based cellular signal sources. Therefore, it will be beneficial to design a hybrid technique that can facilitate location estimation and tracking based on these two types of measurement inputs. Moreover, the performance of the location estimation schemes varies depending on the environmental conditions and the operational parameters. The Cramer–Rao lower bound [14] associated with the geometric dilution of precision (GDOP) [26] is utilized as the theoretical limitation on estimation variance to provide a benchmark for comparison between different estimators. Previous works [22], [27], [28] have been dedicated to combining multiple location techniques for enhanced positioning precision with the theoretical lower bound derived in [27].

In the location tracking problem, the relationship between the measurement and the state variable is observed to be nonlinear. Since the computation of recursive Bayesian estimation requires several integrals without analytic solutions, it is not possible to obtain an optimal solution to this problem in practice. The particle filter [29] has been proposed as a nonlinear/non-Gaussian method for this type of problem. However, the number of particles to establish the probability distribution function should be infinite to achieve the optimal solution. Therefore, in the location tracking problem, there are several methodologies for obtaining the suboptimal solution to deal with the nonlinear relationship between the distance measurement and the estimated position. As shown in the left plot of Fig. 1, the hybrid cascade location tracking (HCLT) scheme proposed in [22] utilizes the two-step LS method [12], [13] for initial location estimation of the MS. The two-stage architecture handles the nonlinear relation in the location estimator. Therefore, the Kalman filtering technique is adopted to smooth out the estimation error by tracking the positions and velocities of the MS. The fusion algorithm is utilized to combine the tracking results from two different sources to obtain the final location estimation of the MS. In the middle plot of Fig. 1, the hybrid Kalman tracking (HKT) scheme extends the Kalman tracking (KT) scheme in [23] by separating the linear components from the originally nonlinear equations for location tracking. The linear aspect is directly processed within the Kalman filtering formulation, whereas the nonlinear term is served as an external measurement input to the Kalman filter. However, both HCLT and HKT algorithms have the drawback of additional hardware cost due to their cascaded infrastructures. The Kalman filter is only utilized to deal with the linear behaviors of location tracking problem by adopting these two types of architectures. The nonlinear terms are considered outside of the Kalman filter by performing LS linearization technique, which can result in information loss and cause larger location tracking errors. This type of structure can result in information loss, which causes larger location tracking errors. Moreover, both algorithms

require sufficient numbers of signal sources from either the TOA or the TDOA path, which cannot resolve the signal insufficiency problem in urban canyons.

In this paper, a hybrid unified KT (HUKT) algorithm is proposed based on both TOA and TDOA signal inputs. Owing to the benefit of a linear relationship between the measurement and estimated states, the Kalman filter is adopted to provide computational efficiency for real-time implementation. As illustrated in the right plot of Fig. 1, the HUKT scheme integrates the nonlinear relation into the Kalman filtering formulation for location tracking based on both TOA and TDOA signal sources from heterogeneous BSs. The major design novelty of the HUKT scheme is that the nonlinear parameters within their respective TOA- and TDOA-based location estimators are mathematically combined into a single state variable, which is to be updated within the Kalman filter. This type of unified architecture for location tracking problem with heterogeneous signal inputs has not been proposed in previous works. In the measurement update of the Kalman filter, the nonlinear parameter is utilized to linearize the measurement equation by assigning all the nonlinear terms into an extra state variable. The constraint between this extra variable and the estimated position is further considered in the state update process of the Kalman filter. The proposed HUKT scheme is feasible to be adopted under environments with heterogeneous signal sources and is tolerant to an insufficient number of BSs from individual signal paths. The determination of the hybrid factor that combines the TOA and TDOA signal sources is investigated based on different criterions. Furthermore, the proposed HUKT algorithm can directly be simplified into a unified KT (UKT) scheme for location tracking under the situation with only homogeneous signal sources, i.e., either the TOA or TDOA measurement input is available. Performance evaluation and comparison of the proposed HUKT and UKT schemes are conducted via simulations. Compared with existing schemes, simulation results show that the HUKT/UKT algorithm can achieve higher accuracy for location estimation and tracking.

The remainder of this paper is organized as follows. The mathematical modeling of signal sources and the existing location tracking techniques are summarized in Section II. Sections III and IV describe the proposed HUKT algorithm and the simplified UKT scheme, respectively. Performance evaluation and comparison of the proposed schemes are conducted in Section V via simulations. Section VI draws our conclusions.

## II. System Modeling and Existing Location Tracking Schemes

### A. Mathematical Modeling of Signal Inputs

In this section, the mathematical models for both TOA and TDOA measurements are presented. The 2-D coordinate of the MS is to be obtained in the proposed HUKT scheme. The TOA measured distance $r_{i,k}$ between the MS and the $i$th BS at the $k$th time step can be represented as

$$r_{i,k} = c \cdot t_{i,k} = \zeta_{i,k} + n_{i,k} + e_{i,k} \quad i = 1, 2, \ldots, N \qquad (1)$$

where $t_{i,k}$ denotes the TOA measurement with respect to the $i$th BS at the $k$th time step, and $c$ is the speed of light. The measured distance $r_{i,k}$ is corrupted by both the measurement noises $n_{i,k}$ and the NLOS error $e_{i,k}$ under urban and suburban areas. The parameter $N$ refers to the total number of TOA measurements. The noiseless distance $\zeta_{i,k}$ in (1) is

$$\zeta_{i,k} = \left[(x_k - x_{i,k})^2 + (y_k - y_{i,k})^2\right]^{1/2} \qquad (2)$$

where $(x_k, y_k)$ represents the MS's true position, and $(x_{i,k}, y_{i,k})$ is the coordinate of the $i$th BS at time step $k$. Based on the preceding TOA signal model, the TDOA measurement can be formulated as the subtraction of two TOA measurements, which conforms to the physical meaning of difference in propagation time. The relative distance $\tilde{r}_{jm,k}$[1] can be obtained by computing the TDOA measurement $\tilde{t}_{jm,k}$, which is the time difference between the MS with respect to the $j$th and $m$th BSs from (1) as

$$\tilde{r}_{jm,k} = c \cdot \tilde{t}_{jm,k} = (\tilde{\zeta}_{j,k} - \tilde{\zeta}_{m,k}) + (\tilde{n}_{j,k} - \tilde{n}_{m,k}) + (\tilde{e}_{j,k} - \tilde{e}_{m,k}) \quad m = 1; j = 2, \ldots, \tilde{N}. \qquad (3)$$

Note that the first BS of the TDOA system is in general denoted as the reference BS, e.g., the serving BS in cellular networks. The TDOA measurements are taken between the reference BS and the other neighbor BSs. The parameter $\tilde{N}$ is the number of BSs for the TDOA system, which comprises $(\tilde{N} - 1)$ independent TDOA measurements.

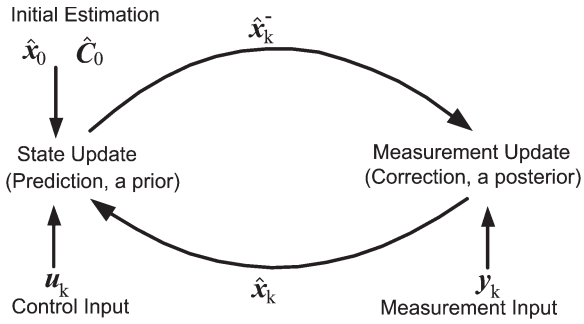


Fig. 2. Schematic diagram of Kalman filter.

### B. Kalman Filter

The Kalman filter [18], [30], which is derived based on the Markov chain perturbed by Gaussian noises, is an efficient Bayesian estimator to solve the linear problem. Fig. 2 illustrates the concept of the Kalman filter that consists of measurement and state updates. With prior information coming from the state update and likelihood information from the measurement update, the Kalman filter will obtain a posterior estimate in the MMSE sense. Even with non-Gaussian noises, the LMMSE solution can still be acquired by adopting the Kalman filter. The

[1] In the paper, it is considered that the TDOA and the TOA measurements come from two different types of networks. For notational convenience, the variables with a tilde are denoted for the measurements from TDOA system, e.g., $\tilde{r}_{jm,k}$; while the variables without the tilde (e.g., $r_{i,k}$) are utilized for TOA measurements.

measurement and state equations for the Kalman filter can be represented as

$$\boldsymbol{y}_k = \mathbf{M}_k \hat{\boldsymbol{x}}_k + \boldsymbol{m}_k \tag{4}$$

$$\hat{\boldsymbol{x}}_k = \mathbf{F}_k \hat{\boldsymbol{x}}_{k-1} + \boldsymbol{u}_{k-1} + \boldsymbol{p}_{k-1} \tag{5}$$

where $\hat{\boldsymbol{x}}_k$ represents the estimated state/output, $\boldsymbol{y}_k$ denotes the measurement input of the Kalman filter, and $\boldsymbol{u}_{k-1}$ indicates the control input for the state model. In the location tracking problem, the states that are of interest include the MS's position, velocity, and acceleration. The matrices $\mathbf{M}_k$ and $\mathbf{F}_k$ refer to the linear relations for the measurement and state models, respectively. The variables $\boldsymbol{m}_k$ and $\boldsymbol{p}_{k-1}$ respectively denote the measurement and the processing noises associated with the covariance matrices $\mathbf{R}_k$ and $\mathbf{Q}_k$ within the Kalman filter formulation. Based on the measurement and state equations as in (4) and (5), the Kalman filter estimates the states during the prediction phase in Fig. 2 as $\hat{\boldsymbol{x}}_k^- = \mathbf{F}_k \hat{\boldsymbol{x}}_{k-1} + \boldsymbol{u}_{k-1}$ with its estimate covariance $\mathbf{C}_k^- = \mathbf{F}_k \mathbf{C}_{k-1} \mathbf{F}_k^{\mathrm{T}} + \mathbf{Q}_k$. On the other hand, within the correction phase, the measurement input will be corrected via innovation process as $\tilde{\boldsymbol{y}}_k = \boldsymbol{y}_k - \mathbf{M}_k \hat{\boldsymbol{x}}_k^-$ with innovation covariance $\tilde{\mathbf{C}}_k = \mathbf{M}_k \mathbf{C}_k^- \mathbf{M}_k^{\mathrm{T}} + \mathbf{R}_k$. The optimal Kalman gain can be obtained as $\mathbf{K}_k = \mathbf{C}_k^- \mathbf{M}_k^{\mathrm{T}} [\tilde{\mathbf{C}}_k]^{-1}$. Therefore, the corrected state estimate will be acquired as $\hat{\boldsymbol{x}}_k = \hat{\boldsymbol{x}}_k^- + \mathbf{K}_k \tilde{\boldsymbol{x}}_k$ associated with the corrected estimate covariance $\mathbf{C}_k = (I - \mathbf{K}_k \mathbf{M}_k) \mathbf{C}_k^-$. Based on the foregoing linear operations, the Kalman filter can efficiently update the state estimates at different time instants.

### C. HCLT Scheme

The left plot of Fig. 1 illustrates the architecture of the HCLT scheme [22]. The HCLT system consists of an LS location estimator, e.g., the two-step LS method, followed by a Kalman filtering technique at the next stage. Different versions of two-step LS methods have been proposed for distinct occasions, such as TOA [12], TDOA [13], and TDOA/AOA [31] measurement inputs. The concept of the two-step LS method is to acquire an intermediate location estimate in the first step with the definition of a new variable to represent the nonlinear term, which is mathematically related to the MS's position. This assumption effectively transforms the nonlinear equations for location estimation into a set of linear equations, which can directly be solved by the LS method. The second step of the method primarily considers the fact that the newly defined variable is related to the MS position, which was originally assumed to be uncorrelated in the first step. An improved location estimate can be obtained after the adjustment from the second step.

The MS's estimated position from the output of the two-step LS estimator will be postprocessed by the Kalman filtering technique according to [17]. The Kalman filter smoothes out and tracks the estimation errors by adopting linear prediction from the previous estimation data while the MS is dynamically moving in the network. According to the Bayesian inference model [15], [32], the tracking results from the two disparate TOA and TDOA paths will be combined by the fusion mechanism based on their corresponding signal variations. The MS's estimated position, i.e., $(\hat{x}_k, \hat{y}_k)$, can therefore be acquired. The detail algorithm of the HCLT scheme can be found in [22].

### D. HKT Scheme

Since the equations associated with the network-based location estimation are inherently nonlinear, different mechanisms, e.g., linearization, are utilized within the existing algorithms for location tracking. The KT scheme [23] considers the nonlinear term as an external measurement input to its Kalman filtering formulation. It distinguishes the linear part from the original nonlinear equations for location estimation and tracking. However, the KT scheme does not specifically indicate the method for acquiring the nonlinear term. For comparison purpose, the KT scheme that was originally proposed based on the TDOA measurement inputs is reformulated and extended in this paper to consider both TOA and TDOA signal sources. The middle plot of Fig. 1 illustrates the architecture of the HKT scheme. The nonlinear terms can be obtained from external location estimators, e.g., by adopting the two-step LS method. With the formulation of the HKT scheme, a feasible accuracy can be acquired for location tracking, including position, velocity, and acceleration of the MS. However, the accuracy is significantly affected by the precision of the external location estimator. The detailed algorithm of the KT scheme can be found in [23].

## III. Proposed Hybrid Unified Kalman Tracking Scheme

The proposed HUKT scheme will be described in this section. The formulation of the HUKT algorithm is explained in Section III-A, and the determination of the hybrid factor $\beta_k$ at time step $k$ will be discussed in Section III-B. The variable $\beta_k$ will be determined from three different approaches to address the various weighting factors between the TOA and TDOA measurements for the HUKT scheme.

### A. Formulation of HUKT Algorithm

The right plot of Fig. 1 illustrates the architecture of the proposed HUKT scheme. Unlike the previous algorithms, e.g., the HCLT and HKT methods, the main design concept of the HUKT scheme is to provide a unified methodology for location estimation and tracking. The purpose of the HUKT algorithm is to obtain the updated state variables via the Kalman filtering technique directly from both TOA and TDOA measurements as the system inputs. The measurement update and the state update equations of the Kalman filter can be respectively acquired from (4) and (5), where $\hat{\boldsymbol{x}}_k = [\hat{x}_k \ \hat{y}_k \ \hat{\Re}_k \ \hat{v}_{x,k} \ \hat{v}_{y,k} \ \hat{a}_{x,k} \ \hat{a}_{y,k}]^T$ is the state vector that includes the MS's estimated position $(\hat{x}_k, \hat{y}_k)$, the estimated velocity $(\hat{v}_{x,k}, \hat{v}_{y,k})$, the estimated acceleration $(\hat{a}_{x,k}, \hat{a}_{y,k})$, and the estimated variable $\hat{\Re}_k$. Note that $\hat{\Re}_k$ represents the estimated nonlinear term for the hybrid location estimation. The updating process of $\hat{\Re}_k$ will be addressed later. To formulate the input/output relationship for Kalman filter based location tracking, error-free measurements will first be examined, i.e., $r_{i,k} = \zeta_{i,k}$. The following equation for TOA measurement can be obtained by combining (1) and (2) as

$$r_{i,k}^2 - K_{i,k} = -2x_{i,k}x_k - 2y_{i,k}y_k + R_k \tag{6}$$

where $K_{i,k} = x_{i,k}^2 + y_{i,k}^2$, and $R_k = x_k^2 + y_k^2$. Similarly, the following relation can also be acquired from the TDOA

measurements (3) by substituting $m = 1$ as

$$\tilde{r}_{j1,k}^2 - (\tilde{K}_{j,k} - \tilde{K}_{1,k}) = -2(\tilde{x}_{j,k} - \tilde{x}_{1,k})x_k - 2(\tilde{y}_{j,k} - \tilde{y}_{1,k})y_k - 2\tilde{r}_{1,k}\tilde{r}_{j1,k} \quad (7)$$

where $\tilde{r}_{1,k}$ indicates the measured distance from the MS to the reference BS via the TDOA system. To design a unified structure for location tracking, the purpose of the proposed HUKT scheme is to obtain an effective method to combine both TOA and TDOA measurements. More specifically, a new variable $\hat{\Re}_k$ is introduced to combine the nonlinear terms $R_k$ in (6) and $\tilde{r}_{1,k}$ in (7). Without loss of generality, the nonlinear term $\tilde{r}_{1,k}$ in (7) can be represented as $\sqrt{x_k^2 + y_k^2}$ by shifting the entire coordinate, i.e., both TOA and TDOA systems, such that $(\tilde{x}_{1,k}, \tilde{y}_{1,k}) = (0, 0)$. With the definition of a hybrid factor $\beta_k$, the following relationship can be obtained by multiplying (7) with $\beta_k/\tilde{r}_{j1,k}$ and adding to (6) as

$$\begin{aligned} r_{i,k}^2 - K_{i,k} + \beta_k\tilde{r}_{j1,k} - \beta_k\frac{\tilde{K}_{j,k} - \tilde{K}_{1,k}}{\tilde{r}_{j1,k}} + \beta_k^2 \\ = \Re_k - 2\left(x_{i,k} + \beta_k\frac{\tilde{x}_{j,k} - \tilde{x}_{1,k}}{\tilde{r}_{j1,k}}\right)x_k \\ - 2\left(y_{i,k} + \beta_k\frac{\tilde{y}_{j,k} - \tilde{y}_{1,k}}{\tilde{r}_{j1,k}}\right)y_k \end{aligned} \quad (8)$$

where $\Re_k = (\sqrt{x_k^2 + y_k^2} - \beta_k)^2$ corresponds to the variable that combines the effects from both TOA and TDOA measurements. It is included in the state vector $\hat{\boldsymbol{x}}_k$ for state updating within the Kalman filtering formulation. The hybrid factor $\beta_k$ is considered as a weighting between the TOA- and TDOA-based measurements, which can be determined according to the signal qualities of the two different paths. The detail design and selection for the value of $\beta_k$ will be addressed later in the next section. Note that (8) is obtained as a linear combination from (6) and (7). Since the Kalman filter is well known for its linear operations, it is not required to apply scaling factors to achieve this combination from two different types of signal sources. As a result, the measurement data $\boldsymbol{y}_k$ and the matrix $\mathbf{M}_k$ associated with the measurement process in (4) can be acquired as in (9), shown at the bottom of the page. Note that there are $(N + \tilde{N} - 2)$ linearly independent equations associated with both $\boldsymbol{y}_k$ and $\mathbf{M}_k$. There are $N$ hybrid equations formed by all the TOA measurements, i.e., from $r_{1,k}$ to $r_{N,k}$, and the first TDOA measurement $\tilde{r}_{21,k}$. The remaining $\tilde{N} - 2$ hybrid equations are established by using the first TOA measurement, i.e., $r_{1,k}$, and the remaining TDOA measurements, i.e., from $\tilde{r}_{31,k}$ to $\tilde{r}_{\tilde{N}1,k}$. Under the assumption of constant acceleration model, the updating process of $\hat{x}_k$ and $\hat{y}_k$ is determined as

$$\hat{x}_k = \hat{x}_{k-1} + \hat{v}_{x,k-1}\Delta t + \frac{1}{2}\hat{a}_{x,k-1}\Delta t^2 \quad (10)$$

$$\hat{y}_k = \hat{y}_{k-1} + \hat{v}_{y,k-1}\Delta t + \frac{1}{2}\hat{a}_{y,k-1}\Delta t^2 \quad (11)$$

where $\Delta t$ denotes the sampling time interval. To provide the updating process for the new variable $\Re_k$, similar to (8), the relation among $\hat{\Re}_k$, $\hat{x}_k$, and $\hat{y}_k$ can be acquired by summing all

$$\boldsymbol{y}_k = \begin{bmatrix} r_{1,k}^2 - K_{1,k} + \beta_k\tilde{r}_{21,k} - \beta_k\frac{\tilde{K}_{2,k} - \tilde{K}_{1,k}}{\tilde{r}_{21,k}} + \beta_k^2 \\ {r_{2,k}}^2 - K_{2,k} + \beta_k\tilde{r}_{21,k} - \beta_k\frac{\tilde{K}_{2,k} - \tilde{K}_{1,k}}{\tilde{r}_{21,k}} + \beta_k^2 \\ \vdots \\ {r_{N,k}}^2 - K_{N,k} + \beta_k\tilde{r}_{21,k} - \beta_k\frac{\tilde{K}_{2,k} - \tilde{K}_{1,k}}{\tilde{r}_{21,k}} + \beta_k^2 \\ r_{1,k}^2 - K_{1,k} + \beta_k\tilde{r}_{31,k} - \beta_k\frac{\tilde{K}_{3,k} - \tilde{K}_{1,k}}{\tilde{r}_{31,k}} + \beta_k^2 \\ r_{1,k}^2 - K_{1,k} + \beta_k\tilde{r}_{41,k} - \beta_k\frac{\tilde{K}_{4,k} - \tilde{K}_{1,k}}{\tilde{r}_{41,k}} + \beta_k^2 \\ \vdots \\ r_{1,k}^2 - K_{1,k} + \beta_k\tilde{r}_{\tilde{N}1,k} - \beta_k\frac{\tilde{K}_{\tilde{N},k} - \tilde{K}_{1,k}}{\tilde{r}_{\tilde{N}1,k}} + \beta_k^2 \end{bmatrix}$$

$$\mathbf{M}_k = \begin{bmatrix} -2\left(x_{1,k} + \beta_k\frac{\tilde{x}_{2,k} - \tilde{x}_{1,k}}{\tilde{r}_{21,k}}\right) & -2\left(y_{1,k} + \beta_k\frac{\tilde{y}_{2,k} - \tilde{y}_{1,k}}{\tilde{r}_{21,k}}\right) & 1 & \mathbf{0}_{1\times 4} \\ -2\left(x_{2,k} + \beta_k\frac{\tilde{x}_{2,k} - \tilde{x}_{1,k}}{\tilde{r}_{21,k}}\right) & -2\left(y_{2,k} + \beta_k\frac{\tilde{y}_{2,k} - \tilde{y}_{1,k}}{\tilde{r}_{21,k}}\right) & 1 & \mathbf{0}_{1\times 4} \\ \vdots & & & \\ -2\left(x_{N,k} + \beta_k\frac{\tilde{x}_{2,k} - \tilde{x}_{1,k}}{\tilde{r}_{21,k}}\right) & -2\left(y_{N,k} + \beta_k\frac{\tilde{y}_{2,k} - \tilde{y}_{1,k}}{\tilde{r}_{21,k}}\right) & 1 & \mathbf{0}_{1\times 4} \\ -2\left(x_{1,k} + \beta_k\frac{\tilde{x}_{3,k} - \tilde{x}_{1,k}}{\tilde{r}_{31,k}}\right) & -2\left(y_{1,k} + \beta_k\frac{\tilde{y}_{3,k} - \tilde{y}_{1,k}}{\tilde{r}_{31,k}}\right) & 1 & \mathbf{0}_{1\times 4} \\ -2\left(x_{1,k} + \beta_k\frac{\tilde{x}_{4,k} - \tilde{x}_{1,k}}{\tilde{r}_{41,k}}\right) & -2\left(y_{1,k} + \beta_k\frac{\tilde{y}_{4,k} - \tilde{y}_{1,k}}{\tilde{r}_{41,k}}\right) & 1 & \mathbf{0}_{1\times 4} \\ \vdots & & & \\ -2\left(x_{1,k} + \beta_k\frac{\tilde{x}_{\tilde{N},k} - \tilde{x}_{1,k}}{\tilde{r}_{\tilde{N}1,k}}\right) & -2\left(y_{1,k} + \beta_k\frac{\tilde{y}_{\tilde{N},k} - \tilde{y}_{1,k}}{\tilde{r}_{\tilde{N}1,k}}\right) & 1 & \mathbf{0}_{1\times 4} \end{bmatrix} \quad (9)$$

$N$ TOA measurements of (6) and $\tilde{N}-1$ TDOA measurements of (7) as

$$\hat{\Re}_k = W_k + 2X_{S,k}\cdot\hat{x}_k + 2Y_{S,k}\cdot\hat{y}_k \tag{12}$$

where

$$W_k = \beta_k^2 + \frac{1}{N}\left(\sum_{i=1}^{N} r_{i,k}^2 - \sum_{i=1}^{N} K_{i,k}\right) + \frac{1}{\sum_{j=2}^{\tilde{N}} \tilde{r}_{j1,k}} \cdot \left[\beta_k \sum_{j=2}^{\tilde{N}} \tilde{r}_{j1,k}^2 - \beta_k \sum_{j=2}^{\tilde{N}} \tilde{K}_{j,k} + \beta_k(\tilde{N}-1)\tilde{K}_{1,k}\right]$$

$$X_{S,k} = \frac{\sum_{i=1}^{N} x_{i,k}}{N} + \frac{\beta_k \sum_{j=2}^{\tilde{N}} (\tilde{x}_{j,k} - \tilde{x}_{1,k})}{\sum_{j=2}^{\tilde{N}} \tilde{r}_{j1,k}}$$

$$Y_{S,k} = \frac{\sum_{i=1}^{N} y_{i,k}}{N} + \frac{\beta_k \sum_{j=2}^{\tilde{N}} (\tilde{y}_{j,k} - \tilde{y}_{1,k})}{\sum_{j=2}^{\tilde{N}} \tilde{r}_{j1,k}}.$$

Following the methodology as in (10) and (11), the updating process for the estimated variable $\hat{\Re}_k$ becomes

$$\begin{aligned}\hat{\Re}_k = {} & \hat{\Re}_{k-1} + 2(X_{S,k} - X_{S,k-1})\hat{x}_{k-1} \\ & + 2(Y_{S,k} - Y_{S,k-1})\hat{y}_{k-1} + 2X_{S,k}\hat{v}_{x,k-1}\Delta t \\ & + 2Y_{S,k}\hat{v}_{y,k-1}\Delta t + X_{S,k}\hat{a}_{x,k-1}\Delta t^2 \\ & + Y_{S,k}\hat{a}_{y,k-1}\Delta t^2 + (W_k - W_{k-1}).\end{aligned} \tag{13}$$

Finally, the state matrix $\mathbf{F}_k$ associated within the state equation in (5) for the proposed HUKT scheme can be obtained as in (14), shown at the bottom of the page. The control input $\boldsymbol{u}_{k-1}$ can also be acquired as

$$\boldsymbol{u}_{k-1} = [\,0 \quad 0 \quad (W_k - W_{k-1}) \quad 0 \quad 0 \quad 0 \quad 0\,]^T. \tag{15}$$

To summarize, the proposed HUKT scheme integrates the measurement inputs from heterogeneous location estimation systems based on a unified Kalman filtering structure. The iterative operations of the Kalman filtering technique primarily consist of processes for state update as prediction and measurement update as correction. The equations for state update are represented as

$$\hat{\boldsymbol{x}}_k^- = \mathbf{F}_k\hat{\boldsymbol{x}}_{k-1} + \boldsymbol{u}_{k-1} \tag{16}$$

$$\mathbf{C}_k^- = \mathbf{F}_k\mathbf{C}_{k-1}\mathbf{F}_k^T + \mathbf{Q}_k. \tag{17}$$

The equations for measurement update become

$$\mathbf{K}_k = \mathbf{C}_k^-\mathbf{M}_k^T\left(\mathbf{M}_k\mathbf{C}_k^-\mathbf{M}_k^T + \mathbf{R}_{\mathrm{TOA},k}^h + \mathbf{R}_{\mathrm{TDOA},k}^h\right)^{-1} \tag{18}$$

$$\hat{\boldsymbol{x}}_k = \hat{\boldsymbol{x}}_k^- + \mathbf{K}_k\left(\boldsymbol{y}_k - \mathbf{M}_k\hat{\boldsymbol{x}}_k^-\right) \tag{19}$$

$$\mathbf{C}_k = \mathbf{C}_k^- - \mathbf{K}_k\mathbf{M}_k\mathbf{C}_k^- \tag{20}$$

where $\mathbf{K}_k$ represents the Kalman gain, and the matrix $\mathbf{C}_k$ is denoted as the estimate error covariance. The covariance matrices associated with the TOA and TDOA measurement update processes for hybrid estimation are respectively represented as $\mathbf{R}_{\mathrm{TOA},k}^h = \mathbf{B}\mathbf{R}_{\mathrm{TOA},k}\mathbf{B}^T$ and $\mathbf{R}_{\mathrm{TDOA},k}^h = \tilde{\mathbf{B}}\mathbf{R}_{\mathrm{TDOA},k}\tilde{\mathbf{B}}^T$, where the matrices $\mathbf{B}$ and $\tilde{\mathbf{B}}$ are established to fulfill the requirement for matrix $\mathbf{M}_k$ in (9), i.e.,

$$\mathbf{B} = \begin{bmatrix}[\mathbf{I}]_{N\times N} \\ [\mathbf{C}]_{(\tilde{N}-2)\times N}\end{bmatrix} = \begin{bmatrix} 1 & 0 & \cdots & 0 \\ 0 & 1 & \cdots & 0 \\ \vdots & \vdots & \ddots & \vdots \\ 0 & 0 & \cdots & 1 \\ 1 & 0 & \cdots & 0 \\ \vdots & & & \\ 1 & 0 & \cdots & 0 \end{bmatrix}$$

$$\tilde{\mathbf{B}} = \begin{bmatrix}[\mathbf{D}]_{(N-1)\times\tilde{N}} \\ [\mathbf{E}]_{(\tilde{N}-1)\times\tilde{N}}\end{bmatrix} = \begin{bmatrix} -1 & 1 & 0 & 0 & \cdots & 0 \\ \vdots & & & & & \\ -1 & 1 & 0 & 0 & \cdots & 0 \\ -1 & 0 & 1 & 0 & \cdots & 0 \\ -1 & 0 & 0 & 1 & \cdots & 0 \\ \vdots & \vdots & \vdots & \vdots & \ddots & \vdots \\ -1 & 0 & 0 & 0 & \cdots & 1 \end{bmatrix}.$$

The corresponding covariance matrices $\mathbf{R}_{\mathrm{TOA},k}$ and $\mathbf{R}_{\mathrm{TDOA},k}$ can respectively be acquired as

$$\mathbf{R}_{\mathrm{TOA},k} = \mathbf{L}_k\mathbf{J}_{h,k}\mathbf{L}_k \tag{21}$$

$$\mathbf{R}_{\mathrm{TDOA},k} = \tilde{\mathbf{L}}_k\tilde{\mathbf{J}}_{h,k}\tilde{\mathbf{L}}_k \tag{22}$$

where $\mathbf{L}_k = \mathrm{diag}\{\zeta_{1,k}, \zeta_{2,k}, \ldots, \zeta_{N,k}\}$, $\mathbf{J}_{h,k} = \mathrm{diag}\{\sigma_{1,k}^2, \sigma_{2,k}^2, \ldots, \sigma_{N,k}^2\}$, $\tilde{\mathbf{L}}_k = \mathrm{diag}\{\tilde{\zeta}_{1,k}, \tilde{\zeta}_{2,k}, \ldots, \tilde{\zeta}_{\tilde{N},k}\}$, and $\tilde{\mathbf{J}}_{h,k} = \mathrm{diag}\{\tilde{\sigma}_{1,k}^2, \tilde{\sigma}_{2,k}^2, \ldots, \tilde{\sigma}_{\tilde{N},k}^2\}$.

### *B. Determination of Hybrid Factor $\beta_k$*

As shown in (8), the hybrid factor $\beta_k$ at time step $k$ is utilized to provide the weighting between the TOA and TDOA measurements to merge these two types of inputs for hybrid location tracking. Therefore, it is essential to develop feasible

$$\mathbf{F}_k = \begin{bmatrix} 1 & 0 & 0 & \Delta t & 0 & \frac{1}{2}\Delta t^2 & 0 \\ 0 & 1 & 0 & 0 & \Delta t & 0 & \frac{1}{2}\Delta t^2 \\ 2(X_{S,k} - X_{S,k-1}) & 2(Y_{S,k} - Y_{S,k-1}) & 1 & 2X_{S,k}\Delta t & 2Y_{S,k}\Delta t & X_{S,k}\Delta t^2 & Y_{S,k}\Delta t^2 \\ 0 & 0 & 0 & 1 & 0 & \Delta t & 0 \\ 0 & 0 & 0 & 0 & 1 & 0 & \Delta t \\ 0 & 0 & 0 & 0 & 0 & 1 & 0 \\ 0 & 0 & 0 & 0 & 0 & 0 & 1 \end{bmatrix} \tag{14}$$

mechanisms that can dynamically adjust the hybrid factor in accordance with the variations of estimation quality in the two signal paths. Note that the sign of the weighting value, i.e., the hybrid factor $\beta_k$, will not be influential based on the design of hybrid system in (8), whereas its magnitude is considered crucial to affect the performance of the hybrid location estimation. With larger absolute value of $\beta_k$, more weighting is assigned to the TDOA signal compared with TOA measurement input. In the following three sections, different types of design for the hybrid factor will be presented.

*GDOP-Based Hybrid Factor (GHF):* The main concept for the design of GHF $\beta_{g,k}$ is to consider the geometric relationship between the TOA and TDOA signal inputs. The GDOP [26] describes the geometry influence on location estimation accuracy. For a set of spatially separated BSs or sensors, the set of relative distances from the MS to its respective BSs affects the estimation accuracy for the MS's position. In general, when the MS locates around the center of the BSs, the GDOP value is lower than the case that the MS is situated around the geometric edge formed by the BSs. Therefore, the GDOP criterion that provides the relative distance information between the MS and BSs can be utilized to determine the hybrid factor $\beta_k$ that represents the weighting between the TOA and TDOA measurements. Considering the MS located at $\boldsymbol{x}_k = (x_k, y_k)$ with the TOA range measurements $r_{i,k}$ for $i = 1$ to $N$ associated with Gaussian noise, the GDOP value $\mathrm{G}_{\boldsymbol{x}_k,\mathrm{TOA}}$ for $\boldsymbol{x}_k$ at time step $k$ can be obtained as

$$\mathrm{G}_{\boldsymbol{x}_k,\mathrm{TOA}} = \left[\mathrm{trace}\left\{\left(\mathbf{H}_{G,k}^T \mathbf{J}_{G,k}^{-1} \mathbf{H}_{G,k}\right)^{-1}\right\}\right]^{1/2} \tag{23}$$

where $\mathbf{J}_{G,k}$ is the same as $\mathbf{J}_{h,k}$ in (21), and

$$\mathbf{H}_{G,k} = \begin{bmatrix} \frac{x_k - x_{1,k}}{r_{1,k}} & \frac{y_k - y_{1,k}}{r_{1,k}} \\ \frac{x_k - x_{2,k}}{r_{2,k}} & \frac{y_k - y_{2,k}}{r_{2,k}} \\ \vdots & \vdots \\ \frac{x_k - x_{N,k}}{r_{N,k}} & \frac{y_k - y_{N,k}}{r_{N,k}} \end{bmatrix}. \tag{24}$$

On the other hand, considering the TDOA case with the range difference measurements $\tilde{r}_{j1,k}$ for $j = 2$ to $\tilde{N}$, the formulation for the GDOP value can be obtained as

$$\mathrm{G}_{\boldsymbol{x}_k,\mathrm{TDOA}} = \left[\mathrm{trace}\left\{\left(\tilde{\mathbf{H}}_{G,k}^T \tilde{\mathbf{J}}_{G,k}^{-1} \tilde{\mathbf{H}}_{G,k}\right)^{-1}\right\}\right]^{1/2} \tag{25}$$

where

$$\tilde{\mathbf{J}}_{G,k} = \begin{bmatrix} \tilde{\sigma}_2^2 + \tilde{\sigma}_1^2 & \tilde{\sigma}_1^2 & \cdots & \tilde{\sigma}_1^2 \\ \tilde{\sigma}_1^2 & \tilde{\sigma}_3^2 + \tilde{\sigma}_1^2 & \cdots & \tilde{\sigma}_1^2 \\ \vdots & \vdots & \ddots & \tilde{\sigma}_1^2 \\ \tilde{\sigma}_1^2 & \tilde{\sigma}_1^2 & \tilde{\sigma}_1^2 & \tilde{\sigma}_{\tilde{N}}^2 + \tilde{\sigma}_1^2 \end{bmatrix} \tag{26}$$

$$\tilde{\mathbf{H}}_{G,k} = \begin{bmatrix} \frac{x-\tilde{x}_2}{\tilde{r}_2} - \frac{x-\tilde{x}_1}{\tilde{r}_1} & \frac{y-\tilde{y}_2}{\tilde{r}_2} - \frac{y-\tilde{y}_1}{\tilde{r}_1} \\ \frac{x-\tilde{x}_3}{\tilde{r}_3} - \frac{x-\tilde{x}_1}{\tilde{r}_1} & \frac{y-\tilde{y}_3}{\tilde{r}_3} - \frac{y-\tilde{y}_1}{\tilde{r}_1} \\ \vdots & \vdots \\ \frac{x-\tilde{x}_{\tilde{N}}}{\tilde{r}_{\tilde{N}}} - \frac{x-\tilde{x}_1}{\tilde{r}_1} & \frac{y-\tilde{y}_{\tilde{N}}}{\tilde{r}_{\tilde{N}}} - \frac{y-\tilde{y}_1}{\tilde{r}_1} \end{bmatrix}. \tag{27}$$

Consequently, the GHF $\beta_{g,k}$ that is designed to be the ratio between the TOA and TDOA estimation systems can be formulated as

$$\beta_{g,k} = \frac{\mathrm{G}_{\boldsymbol{x}_k,\mathrm{TOA}}}{\mathrm{G}_{\boldsymbol{x}_k,\mathrm{TDOA}}} \cdot \tilde{r}_{1,k}. \tag{28}$$

Note that the original TDOA equation in (7) is divided by $\tilde{r}_{i1,k}$ to formulate the hybrid formulation as in (8). Therefore, the multiplication of $\tilde{r}_{1,k}$ in (28) is to scale back to the original magnitude order of the TDOA measurements in (7). For computational simplicity, the value of $\tilde{r}_{1,k}$ is utilized instead of the original $\tilde{r}_{i1,k}$ value. Furthermore, it is noted that both $\mathrm{G}_{\boldsymbol{x}_k,\mathrm{TOA}}$ and $\mathrm{G}_{\boldsymbol{x}_k,\mathrm{TDOA}}$ are nonzero values, which result in a countable value of $\beta_{g,k}$. The case with zero GDOP value denotes that there is no signal variance that is unlikely to happen in realistic estimation problems. On the other hand, when the MS is located exactly on the same location as one of the BSs, singularity will occur in the above matrix operations, which leads to undefined behavior between MS and BSs. Both situations of zero signal variance and matrix singularity will not be considered in this paper.

*Minimum Variance-Based Hybrid Factor (MVHF):* The main purpose of this scheme is to obtain the hybrid factor MVHF $\beta_{m,k}$ to achieve minimum variance for the hybrid estimation system. From the formulation of the HUKT scheme as shown in (8), the hybrid measurement update equation is composed by the TOA measurement from the $i$th BS and the TDOA measurement via the $j$th BS and the serving BS. To facilitate the design of MVHF $\beta_{m,k}$, an equivalent set of BSs is defined as $(x_{eq,k}(i,j), y_{eq,k}(i,j)) = (x_{i,k} + \beta_{m,k}(\tilde{x}_{j,k} - \tilde{x}_{1,k}/\tilde{r}_{j1,k}), y_{i,k} + \beta_{m,k}(\tilde{y}_{j,k} - \tilde{y}_{1,k}/\tilde{r}_{j1,k}))$ for $i = 1$ to $N$ if $j = 2$, and $j = 3$ to $\tilde{N}$ if $i = 1$. Note that there are a total of $N + \tilde{N} - 2$ sets of equivalent BSs. Therefore, the original hybrid measurement update in (8) can be rewritten as

$$\left(\beta_{m,k}\tilde{r}_{j1,k} - \beta_{m,k}\frac{\tilde{K}_{j,k} - \tilde{K}_{1,k}}{\tilde{r}_{j1,k}} + \beta_{m,k}^2 - K_{i,k}\right) + [r_k(i,j)]^2 = -2x_{eq,k}(i,j)x_k - 2y_{eq,k}(i,j)y_k + \Re_k \tag{29}$$

where $r_k(i,j) = r_{i,k}$ for $i = 1$ to $N$ if $j = 2$, and $r_k(i,j) = r_{1,k}$ for $j = 3$ to $\tilde{N}$ if $i = 1$. Note that (29) can be considered as an extended formulation of the TOA measurements in (6). Therefore, it is implicitly suggested by (29) that there exists a set of equivalent BSs $(x_{eq,k}(i,j), y_{eq,k}(i,j))$ for each entry of the hybrid measurement equation, where the equivalent BS is a composition of both TOA and TDOA BSs with the ratio $\beta_{m,k}$, i.e., $(x_{eq,k}(i,j), y_{eq,k}(i,j)) = (x_{i,k} + \beta_{m,k}(\tilde{x}_{j,k} - \tilde{x}_{1,k}/\tilde{r}_{j1,k}), y_{i,k} + \beta_{m,k}(\tilde{y}_{j,k} - \tilde{y}_{1,k}/\tilde{r}_{j1,k}))$.

As a result, the target of MVHF is to acquire an optimal $\beta_{m,k}^*$ such that the variance of the hybrid system can be minimized as

$$\beta_{m,k}^* = \arg \min_{\forall \beta_{m,k} \in \mathbb{R}} \left[\mathrm{trace}\left\{\left(\mathbf{H}_{M,k}^T \mathbf{J}_{M,k}^{-1} \mathbf{H}_{M,k}\right)^{-1}\right\}\right]^{1/2} \tag{30}$$

where

$$\mathbf{H}_{M,k} = \begin{bmatrix} \frac{x_k - x_{eq,k}(1,2)}{r_k(1,2)} & \frac{y_k - y_{eq,k}(1,2)}{r_k(1,2)} \\ \frac{x_k - x_{eq,k}(2,2)}{r_k(2,2)} & \frac{y_k - y_{eq,k}(2,2)}{r_k(2,2)} \\ \vdots & \vdots \\ \frac{x_k - x_{eq,k}(i,j)}{r_k(i,j)} & \frac{y_k - y_{eq,k}(i,j)}{r_k(i,j)} \end{bmatrix} \tag{31}$$

with its rank equal to $(N + \tilde{N} - 2)$. The matrix $\mathbf{J}_{M,k} = \mathbf{R}^h_{\mathrm{TOA},k} + \mathbf{R}^h_{\mathrm{TDOA},k}$ can directly be acquired based on the composition of (21) and (22). Note that the minimization problem in (30) can be interpreted as to search for the variance lower bound for the hybrid tracking system. Moreover, it is recognized that the complicate optimization process in (30) for obtaining $\beta_{m,k}$ will not be feasible for real-time implementation. An alternative method is to perform the numerical search for each specific network layout. For a predetermined BS topology that can be computationally divided by small grids in region, the optimal values of $\beta_{m,k}$ for each grid can be acquired to construct the offline table. Based on the inherent tracking information within the Kalman filter, the predicted *a priori* knowledge of the MS's position will be provided to obtain $\beta_{m,k}$ based on table lookup for real-time implementation.

*Kalman Filter-Based Hybrid Factor (KHF):* As stated in Section III-B1, the design concept of GHF is straightforward, which determines the hybrid factor based on the GDOP values acquired from TOA and TDOA measurements. However, the characteristics of the hybrid structure for location tracking have not been considered in the design of the GHF value. On the other hand, the MVHF designed in Section III-B2 considers the variances of the proposed HUKT system to explore the optimal solution for the hybrid factor. Nevertheless, an approximated solution is obtained due to the complexity of solving the optimization problem in real-time implementation. In this section, the KHF $\beta_{f,k}$ is designed based on the dynamic adjustment of Kalman filtering formulation within the proposed HUKT scheme. It is closely related to the prediction and updating features of the Kalman filter-based location tracking system.

Since the variable $\Re_k$ consists of the hybrid factor and is estimated along with other variables in the state vector, the KHF $\beta_{f,k}$ can also be tracked to further enhance the estimation performance under the presence of measurement errors. Considering the tracking process of the proposed HUKT scheme at the $(k-1)$th time step, the *posteriori* estimation of the state vector can be acquired as $\hat{\boldsymbol{x}}_{k-1} = [\hat{x}_{k-1}\ \hat{y}_{k-1}\ \hat{\Re}_{k-1}\ \hat{v}_{x,k-1}\ \hat{v}_{y,k-1}\ \hat{a}_{x,k-1}\ \hat{a}_{y,k-1}]^T$. The KHF $\beta_{f,k}$ at time step $k$ can be predicted according to the definition of $\hat{\Re}_{k-1}$ in (8) at the $(k-1)$th time step as

$$\beta_{f,k} = \left(\hat{x}^2_{k-1} + \hat{y}^2_{k-1}\right)^{1/2} - (\hat{\Re}_{k-1})^{1/2}. \tag{32}$$

Note that the solution with minus sign is selected in (32) within its multiple solutions for computation simplicity since the sign of $\beta_{f,k}$ is not influential based on the original design of the hybrid system in (8). The proposed KHF $\beta_{f,k}$ can be implemented directly along with the real-time tracking process of the proposed HUKT scheme. In Section V, the performance of location tracking based on these three types of hybrid factor will be evaluated and compared via simulations.

## IV. Simplified Time of Arrival- and Time Difference of Arrival-Based Unified Kalman Tracking Schemes

Considering environments with only a homogeneous type of signal inputs, the proposed HUKT algorithm can be simplified to the UKT scheme to support either TOA or TDOA measurements, i.e., the UKT-TOA and UKT-TDOA schemes. Note that the HUKT algorithm can be adopted under situations where there is insufficient number of measurements at one of the heterogeneous signal paths. With homogeneous signal sources, the MS and network operator that utilize either UKT-TOA or UKT-TDOA technique can have the flexibility to terminate the hybrid estimation mode to reduce computational complexity. In the next two sections, the formulations of both UKT-TOA and UKT-TDOA schemes will be described.

### A. UKT-TOA Scheme

The formulation of the proposed HUKT algorithm can be reduced to the UKT-TOA scheme in the case that there only exists TOA measurements for location estimation and tracking. Based on the rearranged TOA measurements in (6), the same Kalman filter formulation as described in (4) and (5) can still be utilized for measurement and state updates, respectively, where the state vector becomes $\hat{\boldsymbol{x}}_k = [\hat{x}_k\ \hat{y}_k\ \hat{R}_k\ \hat{v}_{x,k}\ \hat{v}_{y,k}\ \hat{a}_{x,k}\ \hat{a}_{y,k}]^T$. Within the state vector, it can be observed that the original nonlinear term $\hat{\Re}_k$ for the hybrid system is substituted into the variable $\hat{R}_k = \hat{x}^2_k + \hat{y}^2_k$, which denotes the nonlinear variable derived from pure TOA-based measurements. Therefore, the measurement data $\boldsymbol{y}_k$ and the matrix $\mathbf{M}_k$ of the $N$ TOA measurements in the measurement update process become

$$\mathbf{y}_k = \begin{bmatrix} r^2_{1,k} - K_{1,k} \\ r^2_{2,k} - K_{2,k} \\ \vdots \\ r^2_{N,k} - K_{N,k} \end{bmatrix}$$

$$\mathbf{M}_k = \begin{bmatrix} -2x_{1,k} & -2y_{1,k} & 1 & \mathbf{0}_{1\times 4} \\ -2x_{2,k} & -2y_{2,k} & 1 & \mathbf{0}_{1\times 4} \\ \vdots & & & \\ -2x_{N,k} & -2y_{N,k} & 1 & \mathbf{0}_{1\times 4} \end{bmatrix}.$$

The covariance matrix $\mathbf{R}_{\mathrm{TOA},k}$ associated with the measurement equation in (4) is obtained from (21). Based on the same assumption of constant acceleration model, the state update process of $\hat{x}_k$ and $\hat{y}_k$ can still be acquired based on (10) and (11). By summing up and rearranging all the $N$ measurement equations, the following relationship can be obtained as

$$\hat{R}_k = W_{T,k} + 2X_{T,k} \cdot \hat{x}_k + 2Y_{T,k} \cdot \hat{y}_k \tag{33}$$

where

$$W_{T,k} = \sum_{i=1}^{N} r^2_{i,k} - \sum_{i=1}^{N} K_{i,k}$$

$$X_{T,k} = \sum_{i=1}^{N} x_{i,k} \quad Y_{T,k} = \sum_{i=1}^{N} y_{i,k}. \tag{34}$$

With (10), (11), and (33), the update process of the state variable $\hat{R}_k$ becomes

$$\begin{aligned}\hat{R}_k =& \hat{R}_{k-1} + 2(X_{T,k} - X_{T,k-1})\hat{x}_{k-1} \\ &+ 2(Y_{T,k} - Y_{T,k-1})\hat{y}_{k-1} + 2X_{T,k}\hat{v}_{x,k-1}\Delta t \\ &+ 2Y_{T,k}\hat{v}_{y,k-1}\Delta t + X_{T,k}\hat{a}_{x,k-1}\Delta t^2 \\ &+ Y_{T,k}\hat{a}_{y,k-1}\Delta t^2 + (W_{T,k} - W_{T,k-1}). \end{aligned} \tag{35}$$

Based on the derivations as above, all of the state variables can be obtained for the UKT-TOA scheme. The matrix $\mathbf{F}_k$ associated with state equation (5) can be expressed by replacing $X_{S,k}$ and $Y_{S,k}$ in (14) with $X_{T,k}$ and $Y_{T,k}$ in (34), respectively, for all $k$. The control input $\boldsymbol{u}_{k-1}$ in (5) can also be acquired by changing $W_k$ in (15) to $W_{T,k}$ for all $k$.

### B. UKT-TDOA Scheme

Under the network scenarios that there only exists TDOA measurement inputs, the UKT-TDOA scheme can be utilized to perform location estimation and tracking for the MS. The formulation of the UKT-TDOA scheme is similar to that of the UKT-TOA method, as stated in the previous section. The major difference is that the third nonlinear state variable in the state vector is replaced by $\hat{r}_{1,k} = [(\hat{x}_k - \tilde{x}_{1,k})^2 + (\hat{x}_k - \tilde{y}_{1,k})^2]^{1/2}$ instead of $\hat{R}_k$ for the UKT-TOA scheme, i.e., the state vector becomes $\hat{\boldsymbol{x}}_k = [\hat{x}_k \ \hat{y}_k \ \hat{r}_{1,k} \ \hat{v}_{x,k} \ \hat{v}_{y,k} \ \hat{a}_{x,k} \ \hat{a}_{y,k}]^T$. Note that the variable $\hat{r}_{1,k}$ represents the estimated distance from the MS to the reference BS based on the TDOA system. With the available $\tilde{N}$ TDOA BSs, there will exist $\tilde{N} - 1$ time difference measurements. Therefore, from (7), the measurement data $\boldsymbol{y}_k$ and the matrix $\mathbf{M}_k$ in (4) can be acquired as shown at the bottom of the page. The covariance matrix $\tilde{\mathbf{R}}_{\mathrm{TDOA},k}$ within the Kalman filter measurement update is the same as (22). Similar to the methodology stated in the UKT-TOA scheme, the state variable $\hat{r}_{1,k}$ can be represented as

$$\hat{r}_{1,k} = W_{D,k} + 2X_{D,k} \cdot \hat{x}_k + 2Y_{D,k} \cdot \hat{y}_k \tag{36}$$

where

$$\begin{aligned} W_{D,k} =& \frac{1}{2\sum_{i=2}^{\tilde{N}} \tilde{r}_{i1,k}} \\ &\times \left[ \sum_{i=2}^{\tilde{N}} \tilde{K}_{i,k} - \sum_{i=2}^{\tilde{N}} \tilde{r}_{i1,k}^2 - (\tilde{N}-1)\tilde{K}_{1,k} \right] \end{aligned} \tag{37}$$

$$X_{D,k} = -\frac{\sum_{i=2}^{\tilde{N}} (\tilde{x}_{i,k} - \tilde{x}_{1,k})}{\sum_{i=2}^{\tilde{N}} \tilde{r}_{i1,k}}$$

$$Y_{D,k} = -\frac{\sum_{i=2}^{\tilde{N}} (\tilde{y}_{i,k} - \tilde{y}_{1,k})}{\sum_{i=2}^{\tilde{N}} \tilde{r}_{i1,k}}. \tag{38}$$

Consequently, based on (10), (11), and (36), the update process of the variable $\hat{r}_{1,k}$ can be obtained as

$$\begin{aligned}\hat{r}_{1,k} =& \hat{r}_{1,k-1} + (X_{D,k} - X_{D,k-1})\hat{x}_{k-1} \\ &+ (Y_{D,k} - Y_{D,k-1})\hat{y}_{k-1} + X_{D,k}\hat{v}_{x,k-1}\Delta t \\ &+ Y_{D,k}\hat{v}_{y,k-1}\Delta t + \frac{1}{2}X_{D,k}\hat{a}_{x,k-1}\Delta t^2 \\ &+ \frac{1}{2}Y_{D,k}\hat{a}_{y,k-1}\Delta t^2 + (W_{D,k} - W_{D,k-1}). \end{aligned} \tag{39}$$

Finally, the state matrix $\mathbf{F}_k$ of (5) can be obtained by substituting $X_{S,k}$ and $Y_{S,k}$ in (14) with $X_{D,k}/2$ and $Y_{D,k}/2$ in (38), respectively. The control input $\mathbf{u}_{k-1}$ in (5) is acquired by replacing $W_k$ in (15) with $W_{D,k}$ in (37) for all $k$. Performance evaluation of both UKT-TOA and UKT-TDOA schemes will be conducted in the next section.

## V. Performance Evaluation

The performances of the proposed HUKT, UKT-TOA, and UKT-TDOA schemes are evaluated via MATLAB simulation platform. Realistic network simulations are performed to follow the models and parameters for practical systems, including TOA signals from the DSRC network and TDOA signals from the cellular network. Ranging schemes are utilized in these network systems to measure the signal arrival time between the MS and BS, which is adopted to align the time frame of received/transmitted packets and to measure the relative distances for positioning purpose. Since system bandwidth is reserved for the ranging schemes in both networks, perfect scheduling for the TOA and TDOA measurements can be assumed in network simulation. Based on the simulation procedure and parameters adopted in [33], the noise models that are utilized in the simulations are described in Section V-A. Performance comparisons of the proposed HUKT scheme under ideal and realistic network scenarios are conducted in Sections V-B and C, respectively. Section V-D describes the performance evaluation of UKT-TOA and UKT-TDOA schemes under homogeneous networks.

### A. Noise Models

Different noise models [33] for the TOA measurements are considered in the simulations. The measurement noise $n_{i,k}$ in (1) is chosen as the zero-mean Gaussian distribution with standard deviation $\sigma$, i.e., $n_{i,k} \sim \mathcal{N}(0, \sigma^2)$, where $\sigma$ will be selected in the following sections based on different network

$$\boldsymbol{y}_k = \begin{bmatrix} \tilde{r}_{21,k}^2 - (\tilde{K}_{2,k} - \tilde{K}_{1,k}) \\ \tilde{r}_{31,k}^2 - (\tilde{K}_{3,k} - \tilde{K}_{1,k}) \\ \vdots \\ \tilde{r}_{\tilde{N}1,k}^2 - (\tilde{K}_{\tilde{N},k} - \tilde{K}_{1,k}) \end{bmatrix}, \quad \mathbf{M}_k = \begin{bmatrix} -2(\tilde{x}_{2,k} - \tilde{x}_{1,k}) & -2(\tilde{y}_{2,k} - \tilde{y}_{1,k}) & -2\tilde{r}_{21,k} & \mathbf{0}_{1\times 4} \\ -2(\tilde{x}_{3,k} - \tilde{x}_{1,k}) & -2(\tilde{y}_{3,k} - \tilde{y}_{1,k}) & -2\tilde{r}_{31,k} & \mathbf{0}_{1\times 4} \\ \vdots & & & \\ -2(\tilde{x}_{\tilde{N},k} - \tilde{x}_{1,k}) & -2(\tilde{y}_{\tilde{N},k} - \tilde{y}_{1,k}) & -2\tilde{r}_{\tilde{N}1,k} & \mathbf{0}_{1\times 4} \end{bmatrix}$$

environments. On the other hand, the NLOS noise $e_{i,k}$ is modeled by an exponential distribution $p_{e_{i,k}}$ as

$$p_{e_{i,k}}(v) = \begin{cases} \frac{1}{\lambda_i} \exp\left(-\frac{v}{\lambda_i}\right), & v > 0 \\ 0, & \text{otherwise} \end{cases} \tag{40}$$

where $\lambda_i = c \cdot \tau_i = c \cdot \tau_m \zeta_i^{\epsilon} \rho$. The parameter $\tau_i$ is the RMS delay spread between the $i$th BS and MS, $\tau_m$ represents the median of $\tau_i$, and $\epsilon$ is the path loss exponent assumed to be 0.5. The shadow fading factor $\rho$ is a lognormal random variable with zero mean, and its standard deviation $\sigma_\rho$ is set to be 4 dB in the simulation. The value of $\tau_m$ will be determined later according to various circumstances.

For the TDOA measurements, since it is formed by the subtraction of two TOA signals, the same parameter set with the TOA noise model is utilized except for the standard deviation of Gaussian noise $\sigma$ and the mean value of the RMS delay spread $\tau_m$. In the hybrid scenario, both values of $\sigma$ and $\tau_m$ for TDOA-based cellular signals are selected to be larger than that of the TOA-based sensor measurements. The reason for selecting larger values in the cellular network is mainly due to the larger communication ranges of the BSs, which will result in higher Gaussian and NLOS errors. Moreover, a constant acceleration model is assumed for the Kalman filter, and the sampling time interval $\Delta t = 1$ s is selected for the total simulation time of 300 s.

### *B. Performance Comparison of HUKT Scheme Under Ideal Network Scenarios*

The effectiveness of the proposed HUKT scheme associated with the three hybrid factors is evaluated in this section. The simulation scenarios for validating the proposed HUKT algorithm are to consider ideal network environments with only Gaussian noises and sufficient signal sources. There are eight BSs deployed as a regular polygon in the network, which includes four TOA and four TDOA measurements, as illustrated in Fig. 3. Within the total 300-s simulation time, it is assumed that the signals from all the BSs can always be received by the MS such that the precision for location tracking will not be affected by different numbers of available BSs. The source of estimation error is restricted to only Gaussian noise for validation purposes. Zero-mean Gaussian distributions each with standard deviation of 60 m $\mathcal{N}(0, 3600)$ and 120 m $\mathcal{N}(0, 14\,400)$ are chosen for TOA and TDOA measurements, respectively.

Fig. 4 shows the performance validation of the proposed HUKT scheme by observing the position errors in each time step associated with their corresponding hybrid factors, i.e., $\beta_{g,k}$, $\beta_{m,k}$, and $\beta_{f,k}$, which are denoted as HUKT-GHF, HUKT-MVHF, and HUKT-KHF schemes. Note that the average position error is defined as $\Delta P_k = \sum_{\forall m} \|\hat{\boldsymbol{x}}_k - \boldsymbol{x}_k\|/m$, where $\boldsymbol{x}_k$ is the MS's true position at time $k$, and $m = 10$ is the number of simulation rounds for each time step in the entire 300-s simulation time. It can be observed from Fig. 4 that the values of GHF $\beta_{g,k}$ vary in a relatively small range compared with the other two hybrid factors since it is only determined by the geometric relationship between the MS and the associated BSs. The GHF $\beta_{g,k}$ cannot completely react to the operating

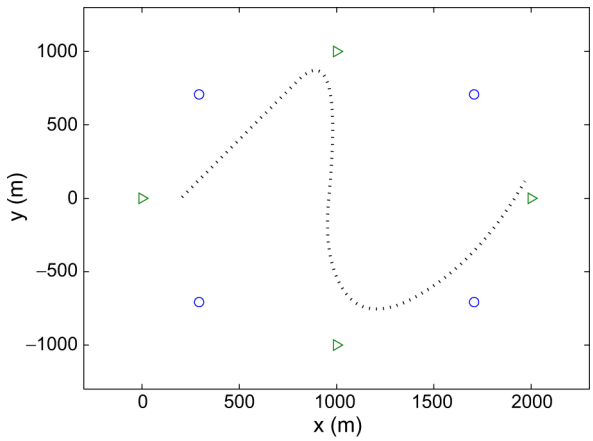


Fig. 3. BS layout and tracking route for the proposed HUKT-GHF, HUKT-MVHF, and HUKT-KHF schemes (triangles: TDOA-based BSs; circles: TOA-based BSs).

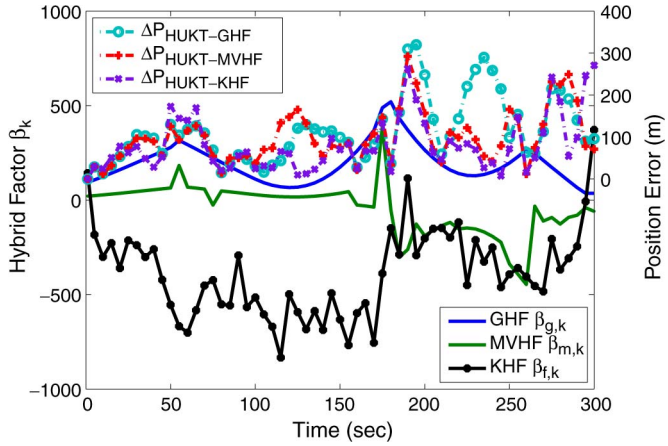


Fig. 4. Position errors associated with the hybrid factors from the proposed HUKT-GHF, HUKT-MVHF, and HUKT-KHF schemes.

status of the proposed HUKT scheme, which results in a larger position error compared with that from the other two hybrid factors $\beta_{m,k}$ and $\beta_{f,k}$. It can be seen that the KHF $\beta_{f,k}$ can quickly respond to variations of position error, e.g., a larger value of $\beta_{f,k}$ is assigned to compensate for the excessive position error at simulation time of around 200 s. Therefore, the proposed HUKT-KHF scheme can provide the smallest average position error of the MS compared with the other two methods.

Fig. 5 illustrates the performance comparison of average position errors among the HCLT algorithm, the HKT method, and the proposed HUKT scheme based on the three determination methods for hybrid factors $\beta_{g,k}$, $\beta_{m,k}$, and $\beta_{f,k}$. Note that the two-step LS method is adopted as the location estimator for both HCLT and HKT schemes, as shown in Fig. 1. It can be seen that the proposed HUKT algorithms outperform the other two existing schemes, e.g., the HUKT-KHF scheme results in around 220 m less in position error compared with the HCLT scheme under 90% average position error. The estimation accuracy for both HCLT and HKT methods relies greatly on the performance of the location estimator. These two-stage location tracking schemes induce larger estimation error compared with the proposed single-stage HUKT algorithm. The nonlinear behavior is also predicted and updated within the

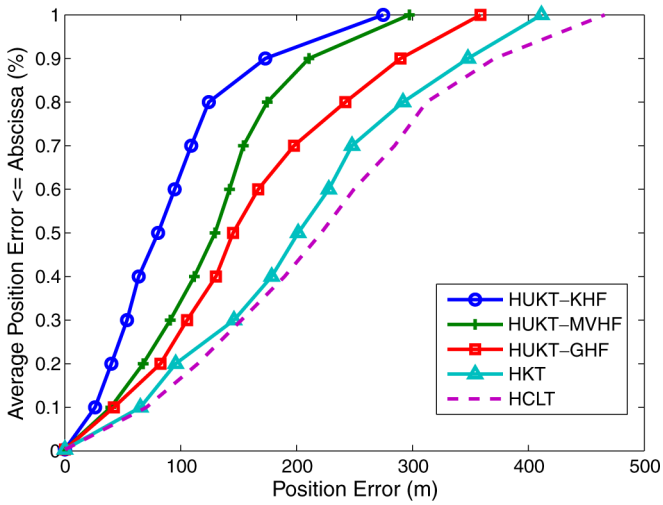


Fig. 5. Performance comparison among the HUKT-GHF, HUKT-MVHF, HUKT-KHF, HKT, and HCLT schemes.

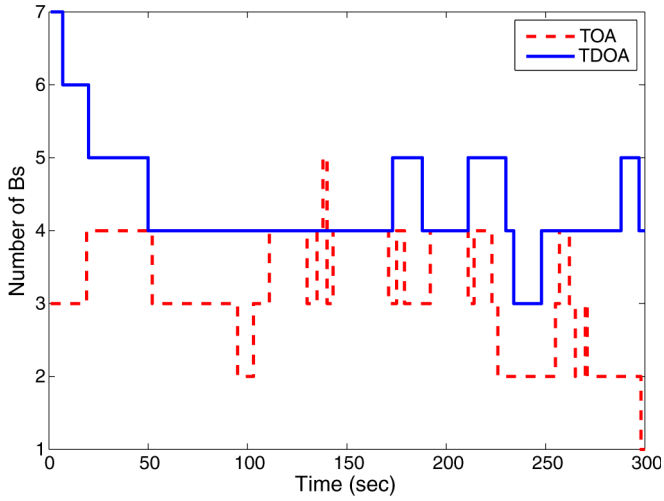


Fig. 6. Number of available BSs from TOA and TDOA measurements.

HUKT formulation, which results in higher location estimation and tracking accuracy for the MS. Furthermore, similar to the observation in Fig. 4, the HUKT-KHF scheme results in the smallest position error in comparison with the HUKT-MVHF and HUKT-GHF methods. The main reason is that the HUKT-KHF algorithm closely follows the KT process for adjusting the hybrid factor $\beta_{f,k}$, which can effectively reduce the tracking error for the MS.

### C. Performance Comparison of HUKT Scheme Under Realistic Network Scenarios

In this section, performance comparisons among HUKT, HKT, and HCLT schemes are implemented under realistic network environments with NLOS noises and insufficient number of signal sources. The network scenario for the simulation is described as follows. As shown in Fig. 9, for MS's location tracking, the BSs deployed in a regular cellular layout are considered to perform TDOA measurements, whereas the randomly distributed short-range sensors conduct TOA measurements. Note that the empty circles represent the locations of the cellular BSs, and the empty triangles indicate the sensor BSs. The noise distributions for the TOA and TDOA measurements are chosen as $\mathcal{N}(0, 3600)$ and $\mathcal{N}(0, 32400)$, i.e., with 60 and 180 m of standard deviation, respectively. The RMS delay spread $\tau_m$ for the NLOS noises is set to be 0.1 for TOA measurements and 0.3 for TDOA measurements. Fig. 6 illustrates the total number of available BSs for TOA and TDOA measurements, respectively, during the simulation time of 300 s. It is noticed that situations with insufficient signal sources are arranged in the simulations, i.e., the number of BSs is less than three and four for TOA and TDOA BSs, respectively.

Fig. 7 shows the position errors along with the corresponding hybrid factors from the proposed HUKT-GHF, HUKT-MVHF, and HUKT-KHF schemes. It can still be observed that the proposed HUKT-KHF scheme outperforms the other two methods under the existence of NLOS noises. Fig. 8 illustrates the performance comparison on the average position errors among HKT, HCLT, and the three proposed HUKT

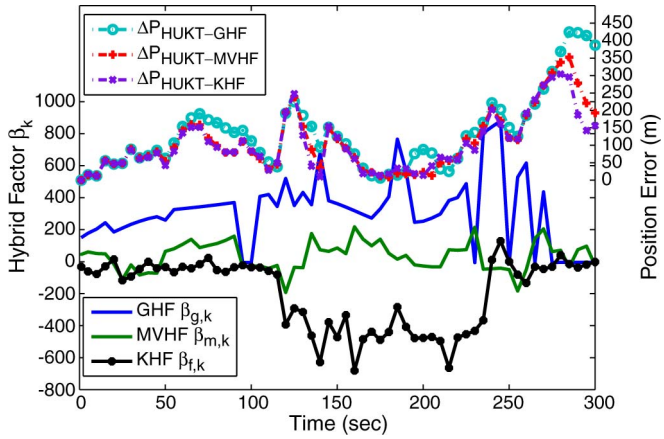


Fig. 7. Position errors associated with the hybrid factors from the proposed HUKT-GHF, HUKT-MVHF, and HUKT-KHF schemes.

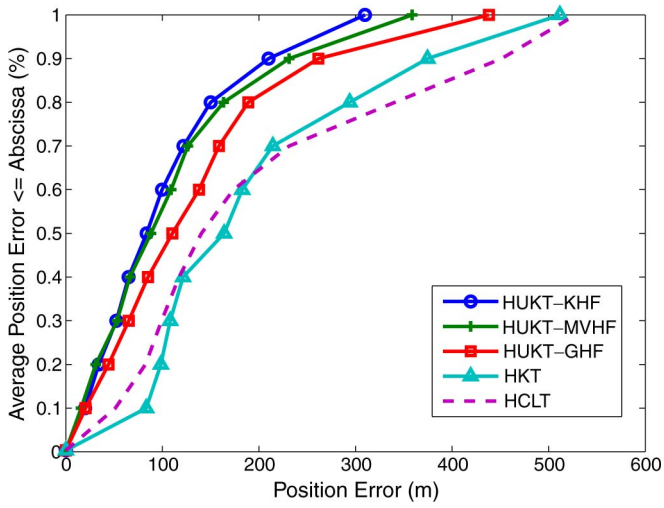


Fig. 8. Performance comparison among the HUKT-GHF, HUKT-MVHF, HUKT-KHF, HKT, and HCLT schemes.

schemes. The proposed HUKT-KHF algorithm can provide better performance compared with all the other schemes, e.g., around 100 m less in position error compared with the HKT and HCLT schemes under 67% average position error. The HUKT

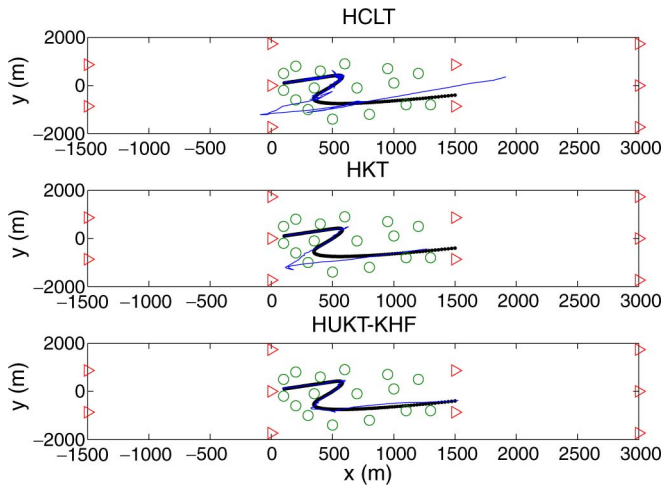


Fig. 9. Trajectory tracking of the MS using the HCLT, HKT, and HUKT-KHF schemes (solid lines: true trajectories; dotted lines: estimated trajectories; triangles: TDOA BSs; circles: TOA BSs).

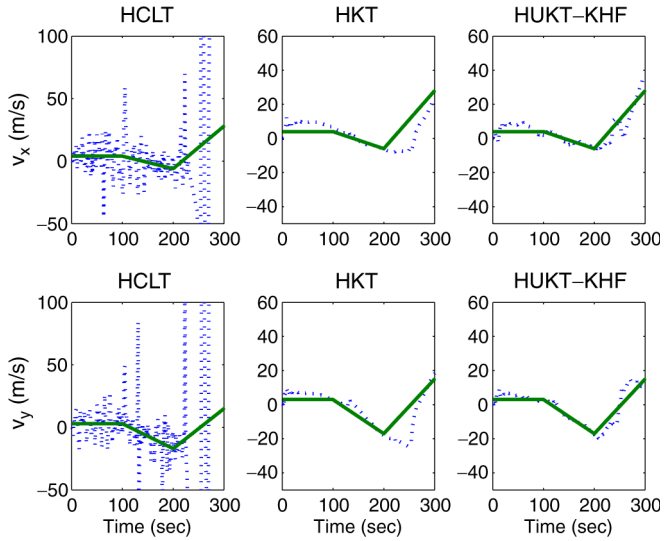


Fig. 10. Velocity tracking of the MS using the HCLT, HKT, and HUKT-KHF schemes (solid lines: true velocities; dotted lines: estimated velocities).

formulation tracks the nonlinear behavior as the information feedback to enhance the measurement update, which results in higher location estimation and tracking accuracy for the MS. Furthermore, the signal insufficiency problem from the individual measurement path can also be alleviated by adopting the proposed HUKT algorithm. Figs. 9–11 show the trajectory tracking for the MS's position, velocity, and acceleration by adopting the HUKT-KHF, HCLT, and HKT schemes. It can be seen that the proposed HUKT-KHF algorithm can provide better tracking capability compared with the other two schemes. Both tracking results obtained from HCLT and HKT schemes severely deviate from their true trajectories as the acceleration has been altered. Furthermore, at the tail of route, the insufficiency of signal sources made both HCLT and HKT algorithms unable to maintain accurate location tracking for the MS. The proposed HUKT-KHF algorithm can still provide consistent performance, including position, velocity, and acceleration, under the variations of MS's mobility.

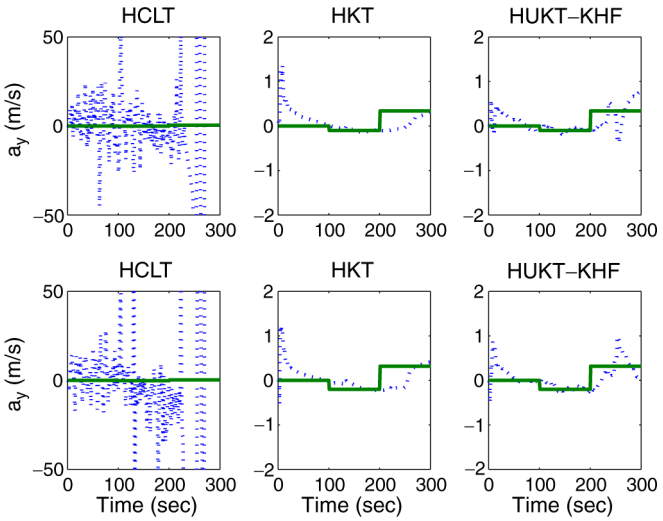


Fig. 11. Acceleration tracking of the MS using the HCLT, HKT, and HUKT-KHF schemes (solid lines: true accelerations; dotted lines: estimated accelerations).

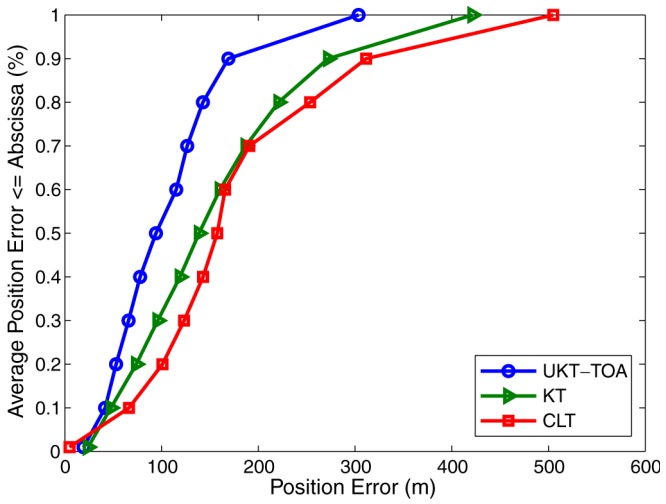


Fig. 12. Performance comparison among the UKT-TOA, KT, and CLT schemes for TOA measurements.

### *D. Performance Comparison of UKT-TOA and UKT-TDOA Schemes*

In this section, the performances of the proposed UKT scheme for pure TOA and TDOA measurement inputs are evaluated. The BSs are designed to locate in the regular cellular layout for both situations. The noise model for both types of signal inputs are Gaussian measurement noises with 60 m standard deviation, i.e., $n_{i,k} \sim \mathcal{N}(0, 3600)$, and exponential NLOS noises as (40) with RMS delay spread $\tau_m = 0.3$. Figs. 12 and 13 respectively show the performance evaluation for the UKT-TOA and UKT-TDOA schemes compared with both KT and cascade location tracking (CLT) algorithms. Note that the KT and CLT schemes are also implemented with pure TOA and TDOA measurement inputs for the purpose of performance comparison.

Similar to the results obtained from the HUKT algorithm, the simplified versions, i.e., the UKT-TOA and UKT-TDOA schemes, can still outperform both KT and CLT algorithms with

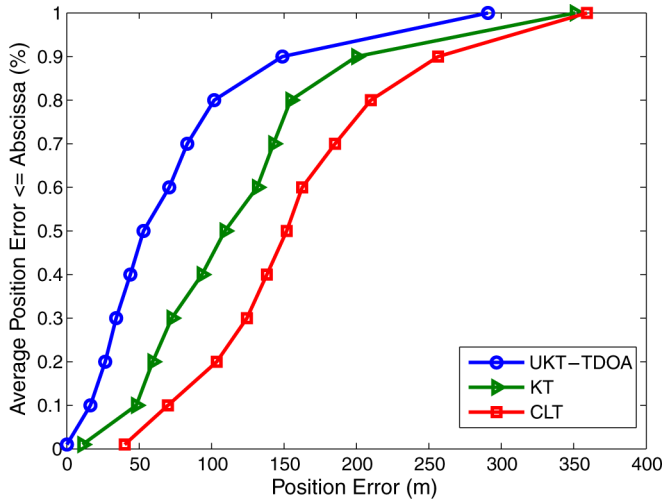


Fig. 13. Performance comparison among the UKT-TDOA, KT, and CLT schemes for TDOA measurements.

homogeneous measurement inputs. For example, as shown in Figs. 12 and 13, under 67% average position error, the proposed UKT-TOA scheme can provide around 60 m less position error compared with the other two methods, whereas the UKT-TDOA algorithm results in 120 m less of position error compared with the CLT scheme. The proposed UKT schemes can additionally track the variation of the nonlinear variable to provide better location tracking accuracy. The effectiveness of the proposed single-stage architecture can be revealed by directly extracting the observation results from original measurement inputs to mitigate the error propagation phenomenon in multiple-stage systems. This benefit of adopting the unified structure for achieving higher precision on location estimation and tracking can therefore be observed.

## VI. Conclusion

In this paper, an HUKT technique has been proposed for location estimation and tracking. Based on heterogeneous signal inputs, the HUKT scheme integrates the location estimation and tracking problems within a unified Kalman filtering formulation. Different hybrid factors are designed for the HUKT algorithm to enhance the location tracking accuracy. Compared with other existing wireless location techniques, simulation results show that the proposed HUKT scheme can both provide higher precision for mobile location tracking and adapt to environments with insufficient signal sources.

## References

[1] C.-T. Chiang, P.-H. Tseng, and K.-T. Feng, "Hybrid TOA/TDOA based unified Kalman tracking algorithm for wireless networks," in *Proc. IEEE Int. Symp. Pers., Indoor Mobile Radio Commun.*, Sep. 2010, pp. 1707–1712.

[2] Federal Communication Commission, *Enhanced 911—Wireless Services*. [Online]. Available: http://www.fcc.gov/911/enhanced/

[3] S. Feng and C. L. Law, "Assisted GPS and its impact on navigation in intelligent transportation systems," in *Proc. IEEE 5th Int. Conf. Intell. Transp. Syst.*, 2002, pp. 926–931.

[4] Y. Zhao, "Standardization of mobile phone positioning for 3G systems," *IEEE Commun. Mag.*, vol. 40, no. 7, pp. 108–116, Jul. 2002.

[5] N. Patwari, J. N. Ash, S. Kyperountas, A. O. Hero, III, R. L. Moses, and N. S. Correal, "Locating the nodes: Cooperative localization in wireless sensor networks," *IEEE Signal Process. Mag.*, vol. 22, no. 4, pp. 54–69, Jul. 2005.

[6] S. Gezici, Z. Tian, G. B. Giannakis, H. Kobayashi, A. F. Molisch, H. V. Poor, and Z. Sahinoglu, "Localization via ultra-wideband radios: A look at positioning aspects for future sensor network," *IEEE Signal Process. Mag.*, vol. 22, no. 4, pp. 70–84, Jul. 2005.

[7] T. He, C. Huang, B. M. Blum, J. A. Stankovic, and T. F. Abdelzaher, "Range-free localization schemes in large scale sensor networks," in *Proc. Int. Conf. Mobile Comput. Netw.*, Sep. 2003, pp. 81–95.

[8] D. Niculescu and B. Nath, "DV based positioning in ad hoc networks," *J. Telecommun. Syst.*, vol. 22, no. 1, pp. 267–280, Jan. 2003.

[9] N. Bulusu, J. Heidemann, and D. Estrin, "Adaptive beacon placement," in *Proc. IEEE Int. Conf. Distrib. Comput. Syst.*, Apr. 2001, pp. 489–498.

[10] A. J. Weiss, "On the accuracy of a cellular location system based on RSS measurements," *IEEE Trans. Veh. Technol.*, vol. 52, no. 6, pp. 1508–1518, Nov. 2003.

[11] G. G. Raleigh and T. Boros, "Joint space-time parameter estimation for wireless communication channels," *IEEE Trans. Signal Process.*, vol. 46, no. 5, pp. 1333–1343, May 1998.

[12] X. Wang, Z. Wang, and B. O'Dea, "TOA-based location algorithm reducing the errors due to non-line-of-sight (NLOS) propagation," *IEEE Trans. Veh. Technol.*, vol. 52, no. 1, pp. 112–116, Jan. 2003.

[13] Y. T. Chan and K. C. Ho, "A simple and efficient estimator for hyperbolic location," *IEEE Trans. Signal Process.*, vol. 42, no. 8, pp. 1905–1915, Aug. 1994.

[14] S. M. Kay, *Fundamentals of Statistical Signal Processing*. Englewood Cliffs, NJ: Prentice-Hall, 1993.

[15] G. R. Iverson, *Bayesian Statistical Inference*. Beverly Hills, CA: Sage, 1984.

[16] S. Haykin, *Adaptive Filter Theory*. Englewood Cliffs, NJ: Prentice–Hall, 2002.

[17] R. E. Kalman, "A new approach to linear filtering and prediction problems," *IEEE/ASME Trans. Mechatron.*, vol. 82, pp. 35–45, Mar. 1960.

[18] G. Welch and G. Bishop, *An Introduction to the Kalman Filter*. Chapel Hill, NC: Dept. Comp. Sci., Univ. North Carolina, 2006.

[19] P.-H. Tseng and K.-T. Feng, "Hybrid network/satellite-based location estimation and tracking systems for wireless networks," *IEEE Trans. Veh. Technol.*, vol. 58, no. 9, pp. 5174–5189, Nov. 2009.

[20] P.-H. Tseng, K.-T. Feng, Y.-C. Lin, and C.-L. Chen, "Wireless location tracking algorithms for environments with insufficient signal sources," *IEEE Trans. Mobile Comput.*, vol. 8, no. 12, pp. 1676–1689, Dec. 2009.

[21] M. Najar and J. Vidal, "Kalman tracking for mobile location in NLOS situations," in *Proc. IEEE International Symposium on Personal, Indoor and Mobile Radio Communications*, Sep. 2003, vol. 3, pp. 2203–2207.

[22] C. L. Chen and K. T. Feng, "Hybrid location estimation and tracking system for mobile devices," in *Proc. IEEE Veh. Technol. Conf.*, Jun. 2005, vol. 4, pp. 2648–2652.

[23] M. Najar and J. Vidal, "Kalman tracking based on TDOA for UMTS mobile location," in *Proc. IEEE Int. Symp. Pers., Indoor Mobile Radio Commun.*, Sep. 2001, vol. 1, pp. B-45–B-49.

[24] *IEEE Standard for Local and Metropolitan Area Networks—Part 16: Air Interference for Fixed Broadband Wireless Access Systems, Amendment 2: Physical and Medium Access Control Layers for Combined Fixed and Mobile Operation in Licensed Bands and Corrigendum 1*, IEEE Std. 802.16e-2005, Dec. 2006.

[25] N. Alam, A. T. Balaei, and A. G. Dempster, "Range and range-rate measurements using DSRC: Facts and challenges," in *Proc. Int. Global Navig. Satellite Syst. Soc.*, Dec. 2009, pp. 1–14.

[26] N. Levanon, "Lowest GDOP in 2-D scenarios," *Proc. Inst. Elect. Eng.—Radar, Sonar Navig.*, vol. 147, no. 3, pp. 149–155, Jun. 2000.

[27] Z. Sahinoglu and A. Catovic, "A hybrid location estimation scheme (H-LES) for partially synchronized wireless sensor networks," in *Proc. IEEE Int. Conf. Commun.*, Jun. 2004, vol. 7, pp. 3797–3801.

[28] A. Broumandan, T. Lin, J. Nielsen, and G. Lachapelle, "Practical results of hybrid AOA/TDOA geo-location estimation in CDMA wireless networks," in *Proc. IEEE Veh. Technol. Conf.*, Sep. 2008, pp. 1–5.

[29] M. S. Arulampalam, S. Maskell, N. Gordon, and T. Clapp, "A tutorial on particle filters for online nonlinear/non-Gaussian bayesian tracking," *IEEE Trans. Signal Process.*, vol. 50, no. 2, pp. 174–188, Feb. 2002.

[30] M. J. Goris, D. A. Gray, and I. M. Y. Mareels, "Reducing the computational load of a Kalman filter," *IEE Electron. Lett.*, vol. 33, no. 18, pp. 1539–1541, Aug. 1997.

[31] L. Cong and W. Zhuang, "Hybrid TDOA/AOA mobile user location for wideband CDMA cellular systems," *IEEE Trans. Wireless Commun.*, vol. 1, no. 3, pp. 439–447, Jul. 2002.

[32] T. K-Ostmann and A. E. Bell, "A data fusion architecture for enhanced position estimation in wireless networks," *IEEE Commun. Lett.*, vol. 5, no. 8, pp. 343–345, Aug. 2001.
[33] P. C. Chen, "A non-line-of-sight error mitigation algorithm in location estimation," in *Proc. IEEE Wireless Commun. Netw. Conf.*, Sep. 1999, vol. 1, pp. 316–320.

**Cheng-Tse Chiang** received the B.S. degree in communication engineering and the M.S. degree from the National Chiao Tung University, Hsinchu, Taiwan, in 2008 and 2010, respectively.

He is currently with Realtek Semiconductor Corp., Hsinchu. His research interests include network protocol design for mobile ad hoc networks, wireless sensor networks, and wireless location estimation and tracking technologies.

**Po-Hsuan Tseng** (S'08) received the B.S. and Ph.D. degrees in communication engineering from the National Chiao Tung University, Hsinchu, Taiwan, in 2005 and 2011, respectively.

He is currently in the military service, Taiwan. From January 2010 to October 2010, he was a Visiting Researcher with the University of California at Davis. His research interests are in the areas of signal processing for networking and communications, including location estimation and tracking, cooperative localization, and mobile broadband wireless access system design.

**Kai-Ten Feng** (M'03) received the B.S. degree from the National Taiwan University, Taipei, Taiwan, in 1992, the M.S. degree from the University of Michigan, Ann Arbor, in 1996, and the Ph.D. degree from the University of California, Berkeley, in 2000.

Between 2000 and 2003, he was an In-Vehicle Development Manager/Senior Technologist with OnStar Corporation, a subsidiary of General Motors Corporation, where he worked on the design of future Telematics platforms and in-vehicle networks. Since August 2007, he has been an Associate Professor with the Department of Electrical Engineering, National Chiao Tung University (NCTU), Hsinchu, Taiwan, where he was an Assistant Professor from August 2007 to July 2011 and from February 2003 and July 2007, respectively. From July 2009 to March 2010, he was a Visiting Scholar with the Department of Electrical and Computer Engineering, University of California at Davis. He has also been the Convener of the NCTU Leadership Development Program since August 2011. Since August 2011, he has been a full Professor with the Department of Electrical Engineering, National Chiao Tung University (NCTU), Hsinchu, Taiwan, where he was an Associate Professor and Assistant Professor from August 2007 to July 2011 and from February 2003 to July 2007, respectively. Since October 2011, he has been serving as the Director of the Digital Content Production Center at the same university. His current research interests include broadband wireless networks, cooperative and cognitive networks, smart phone and embedded system designs, wireless location technologies, and intelligent transportation systems.

Dr. Feng received the Best Paper Award from the Spring 2006 IEEE Vehicular Technology Conference, which ranked his paper first among the 615 accepted papers. He also received the Outstanding Youth Electrical Engineer Award in 2007 from the Chinese Institute of Electrical Engineering and the Distinguished Researcher Award from NCTU in 2008, 2010, and 2011. He has served on the technical program committees of the Vehicular Technology, International Communications, and Wireless Communications and Networking Conferences.